



PAPER

Characteristics of 2D ZnO-based piezoelectric nanogenerator and its application in non-destructive material discrimination

To cite this article: P Supraja *et al* 2021 *Adv. Nat. Sci: Nanosci. Nanotechnol.* **12** 025011

View the [article online](#) for updates and enhancements.

You may also like

- [Electrochemical Impedance Spectroscopy Study of Ni-Ce-Zr-Tb Anode Solid Oxide Fuel Cell Operated with Simulated Biogas](#)
Maria José Escudero, M^a Pilar Yeste Sigüenza, Miguel Angel Cauqui et al.
- [Application of Flexible Catalysts Based on Nickel-Iron Coatings for Overall Water Splitting](#)
Eugenijus Norkus, Dmytro Shyshkin, Birut Šimknaite-Stanykien et al.
- [Corrosion Behavior of Chromium in Molten Carbonate](#)
J. P. T. Vossen, R. C. Makkus and J. H. W. de Wit

Characteristics of 2D ZnO-based piezoelectric nanogenerator and its application in non-destructive material discrimination

P Supraja¹, P Ravi Sankar², R Rakesh Kumar¹, K Prakash², N Jayarambabu¹ and T Venkatappa Rao¹

¹Department of Physics, Nanomaterials and Energy Harvesting Research Lab, National Institute of Technology-Warangal, Telangana, India

²Department of Electronics and Communication Engineering, Flexible Electronics Lab, National Institute of Technology-Warangal, Telangana, India

E-mail: rakeshr@nitw.ac.in

Received 17 November 2020

Accepted for publication 1 April 2021

Published 14 June 2021



CrossMark

Abstract

The present report aims at the application of piezoelectric nanogenerators for non-destructive material discrimination. The detailed characteristics of zinc oxide (ZnO) nanosheet-based piezoelectric nanogenerator and its applications in mechanical energy harvesting and sensing are considered as major objectives of the present study. The nanogenerator is fabricated with ZnO nanosheet film prepared by hydrothermal method with necessary electrodes. The nanogenerator response as a function of different load resistances, different finger-tapping frequencies, different finger-tapping pressures, bending and twisting movements are recorded. The maximum output power of 18 nW is observed at the load resistance of 200 K Ω with 60 mV output voltage. The output voltages of \sim 150 mV, 350 mV, and 200 mV are observed for finger-tapping, bending, and twisting movements, respectively. The output voltages of \sim 76 mV, 100 mV, and 145 mV are observed for low, medium, and high pressures applied by the finger. Nanogenerator is also tested for its stability of the output at different points of time after the device fabrication and found stable over for one year. Further, the nanogenerator is used as an impact sensor for non-destructive material discrimination application. The output voltages of 176 mV, 225 mV, 272 mV, and 300 mV were observed for acrylic, ceramic, marble, glass balls of uniform diameter but with a different mass. The fabricated nanogenerator can discriminate the equal size materials of different densities. Further, ZnO nanosheet-based nanogenerator has potential applications in mechanical sensors due to the high flexibility and mechanical reliability of the ZnO nanosheets.

Keywords: ZnO, sensing, energy harvesting, nanogenerator, nanomaterials

Classification numbers: 2.00, 4.00, 5.03, 6.00, 6.08

1. Introduction

Energy harvesting technologies such as solar, thermal, mechanical have attracted much attention due to the limited availability of non-renewable resources/fossil fuels, environment pollution by fossil fuel usage, and increase in energy demand [1–3]. Among all, mechanical energy harvesting is more attractive due to the easy availability of

mechanical energy everywhere and all the time. The most utilised phenomenon used for mechanical energy harvesting is the piezoelectric effect [4]. In the piezoelectric effect, mechanical deformation along a particular direction induces electrical potential in the piezoelectric material. The piezoelectric effect has been used in many sensing applications like touch, pressure, strain, force, vibration of systems, operating frequency measurement. A wide range of piezoelectric

materials are used to capture mechanical energy in bulk and nanomaterial form, namely lead zirconium titanate (PZT) [5], barium titanite (BaTiO_3) [6], zinc oxide (ZnO) [7], gallium nitrate (GaN) [8], zinc sulfide (ZnS) [9], and polyvinylidene fluoride (PVDF) polymer [10]. Among all, ZnO is the most promising material due to its non-toxicity, cost-effectiveness, easy synthesis in nanomaterial form, the formation of a variety of nanostructures, and good sensing properties [11–13]. The ZnO nanowire-based piezoelectric nanogenerator (PENG) was first reported by the Z L Wang research group [14]. Since then, much attention has been given to the development of nanogenerators for mechanical energy harvesting. Significant research has been published on the ZnO nanorod-based, nanowire-based nanogenerators in the literature [12, 15]. ZnO-based nanogenerator significant potential was demonstrated as various self-powered sensors [16–18]. However, there are very limited studies available on two-dimensional (2D) ZnO nanosheet-based nanogenerators in the literature [19–24]. However, these reports did not carry out a detailed characterisation of nanogenerators such as output behaviour with different load resistances, different frequencies of applied force, different magnitudes of the applied force, and stability of the nanogenerator over a period of time and a large number of cyclic tests. In addition to the above, ZnO nanosheet-based nanogenerator was not explored for material discrimination application as of now. Our research group also reported the flexible nanogenerator based on ZnO nanosheets recently with simple apparatus with a cost-effective method [7]. In our previous report, fabrication of nanogenerator and verification of output voltage by various confirmation tests were reported. In this report, a detailed analysis of ZnO nanosheet-based nanogenerator characteristics will be presented.

Material discrimination plays a significant role in material processing industries and plants [25]. The existing techniques, such as acoustic pulses [26], spectral X-ray imaging [27], optical spectroscopy techniques [28], are expensive, time-consuming, require sophisticated instruments and a trained person. The existing techniques are not suitable for regular laboratory experiments, medium and small-scale industries. Among various applications of nanogenerators, material discrimination by nanogenerators was not explored till now in the literature to the best of the authors' knowledge. However, ZnO thin film impact sensor was demonstrated for non-destructive material discrimination in literature [25]. In this report, expensive RF reactive magnetron sputtering for ZnO thin film deposition and thermal evaporation for top electrode deposition were used. The plane ZnO thin film is prone to cracks under repeated impacts and bending, which leads to failure of the device. In the present manuscript, a low-cost hydrothermal method was employed for ZnO nanosheet synthesis compared to the literature [25]. The ZnO nanosheet film is highly stable and has high mechanical strength under repeated impacts and bending. The ZnO nanosheets' high stability is attributed to the morphologically networked ZnO nanosheets and the high mechanical strength of nanosheets [21].

The present manuscript reports the non-destructive and straight-forward method for material discrimination using a nanogenerator to overcome the above difficulties. In this manuscript, a detailed study of nanogenerator characteristics such as output behaviour with different load resistances, different frequencies of applied force, different magnitudes of the applied force, and long-term stability tests is reported. Further, nanogenerator is demonstrated for material discrimination application based on their densities and pressure sensing application.

2. Experimental

2.1. Materials and methods

The experimental procedure of ZnO nanosheets on aluminium substrates is similar to our previous reports [7, 29]. Clean aluminium substrates (2 cm by 3 cm) were placed over the equimolar solution mixture of zinc nitrate hexahydrate ($\text{Zn}(\text{NO}_3)_2 \cdot 6\text{H}_2\text{O}$) and hexamethylenetetramine (HMTA, $\text{C}_6\text{H}_{12}\text{N}_4$) in a glass beaker. The small portion of the substrate was masked with Kapton tape for the bottom electrode purpose for the device fabrication. The glass beaker was sealed with aluminium foil and kept inside a laboratory oven at 80°C for 4 h to achieve ZnO nanosheet growth. Substrates were removed from the growth solution after 4 h and rinsed with de-ionised water, then dried with a blower. A scanning electron microscope (SEM, VEGA3 TESCAN) was used to study the surface morphology of the obtained thin films on the substrates. The SEM images were captured with a secondary electron detector at a working distance of 9 mm and an accelerating voltage of 10 kV. A transmission electron microscope (TEM, Thermo Fisher, Talos F200 S) was used to study the individual ZnO nanosheet size, microstructure, crystallinity, and composition.

2.2. Nanogenerator device fabrication

The aluminium substrate masked portion was removed and used as the bottom electrode for the device fabrication. The nanogenerator device was fabricated by placing indium tin oxide (ITO) coated polyethylene terephthalate (PET) on the ZnO nanosheets without any short-circuit with the bottom electrode. Copper connecting wires were connected to the bottom aluminium and top ITO electrode. The fabricated nanogenerator device was sealed with a Kapton tape to avoid external static charge and discharges in the testing process. The schematics of the fabricated nanogenerator device and original fabricated devices are shown in figures 1(a) and (b), respectively. The fabricated nanogenerator was tested against different mechanical forces. The nanogenerator's response (open circuit voltage) was recorded with Tektronix-digital storage oscilloscope interfaced with the computer using the KickStart software.

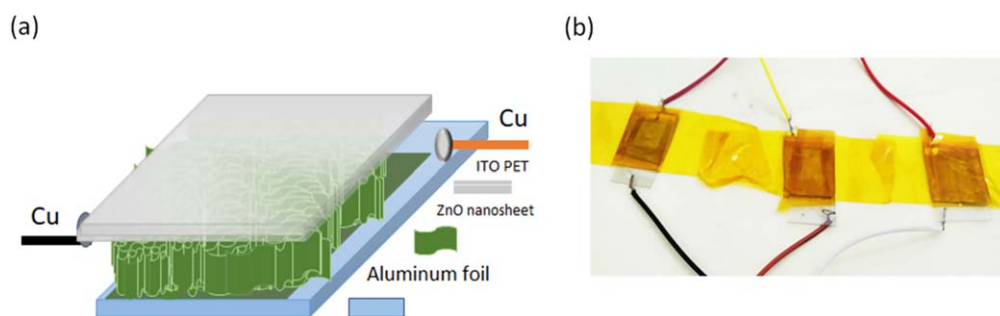


Figure 1. (a) Schematic of the fabricated nanogenerator device, (b) Three nanogenerator devices prepared with the ZnO nanosheet films grown under identical conditions.

2.3. Material discrimination experimental setup

The homemade experimental setup was used for the material discrimination application. In this setup, a hollow pipe is held vertically with a retort stand, and PENG is placed at the bottom end of the hollow pipe on the base plate. In this testing procedure, the same diameter balls made up of different materials were dropped from a constant height through a hollow pipe onto the nanogenerator. The response of the nanogenerator voltage was recorded using a digital storage oscilloscope for every drop test. Four experiments (drop tests) were performed for each ball impact, and the average value of the output voltage was calculated. Details of the balls such as diameter, weights are given in table 1.

3. Results and discussion

The morphology of the obtained ZnO nanosheet networks grown on the aluminium substrate is shown in figure 2(a). A uniform and dense nanosheet network is formed on the substrate. Individual ZnO nanosheet size, microstructure, crystallinity, and composition were studied by TEM. High magnification TEM images of individual ZnO nanosheets are shown in figures 2(b)–(c), confirming the 2D nature of ZnO nanosheets. The size of the nanosheets is in the range of 0.5–1 μm . The high-resolution TEM (HR-TEM) image and selected area electron diffraction (SAED) pattern recorded on the single ZnO nanosheet are shown in figures 2(d)–(e). The HRTEM and SAED confirm the polycrystalline nature of the nanosheets. The lattice spacing of a nanosheet is determined from the inset of figure 2(e) and found 0.289 nm of the wurtzite ZnO. The crystallinity of the ZnO nanosheets was affected by the irradiation damage by the electron beam. The electron beam's irradiation damage of ZnO nanosheets is similar to the reported literature [29–31]. Figure 2(f) shows the EDX spectrum recorded on individual ZnO nanosheets. The EDX spectrum confirms the presence of Zn, O, Al elements, and the presence of Al reveals that the ZnO nanosheets were doped with aluminium, which is similar to the reported literature [32, 33].

The detailed characterisation of ZnO nanosheets and the nanogenerator output voltage's confirmation tests can be found in the previous report [7]. Figure 3(a) shows the piezoelectric nanogenerator (PENG) response with repeated

Table 1. Details of the different balls used for the ball drop test.

Sl. No.	Material type	Diameter (mm)	Weight (gm)
1	Glass	13	3.3
2	Marble	13	3.0
3	Ceramic	13	2.4
4	Acrylic	13	1.4

finger tapping under an open circuit and different external load (R_L) conditions. A maximum output voltage of ~ 150 mV is observed for finger tapping under open-circuit conditions. To find out the maximum output power of the PENG, the variation of piezoelectric output voltage under different external loads ranging from 20 K Ω –100 M Ω is recorded under constant finger tapping pressure. Figure 3(b) shows the variation of the average value of output voltage under different external load conditions. The output voltage is increasing with the increase of load resistance. The saturation of output voltage is observed at higher load resistances of 10 M Ω and above. The saturated value of output voltage at higher resistance is near to the open-circuit voltage. Similar behaviour of nanogenerators was reported earlier in the literature [34, 35].

The power of the PENG device is defined as $P = V^2/R_L$ where V is the output voltage and R_L is load resistance. The variation of the output power of the PENG with external load resistance is shown in figure 3(c). The maximum output power of 18 nW was obtained at the load resistance of 200 Kohms with 60 mV output voltage. The power density values reported in the literature were 37, 50 nWcm $^{-2}$ for a few nanogenerators [36, 37], and 0.6, 2.4, 11.8 μWm^{-2} for other nanogenerators [22, 24, 38]. The power density obtained in the present work 12 nWcm $^{-2}$ is lower compared to the literature. The variation in the power density values for 2D ZnO may be due to the difference in the morphology, different areas of the devices, and different applied forces.

Mechanical energy harvesting of PENG was tested for bending and twisting movements. The response of the PENG for bending and twisting motions is shown in figures 4(a)–(b). The output voltages of ~ 350 mV and 200 mV were observed for bending and twisting movements of the device. The high output voltage for bending PENG is associated with

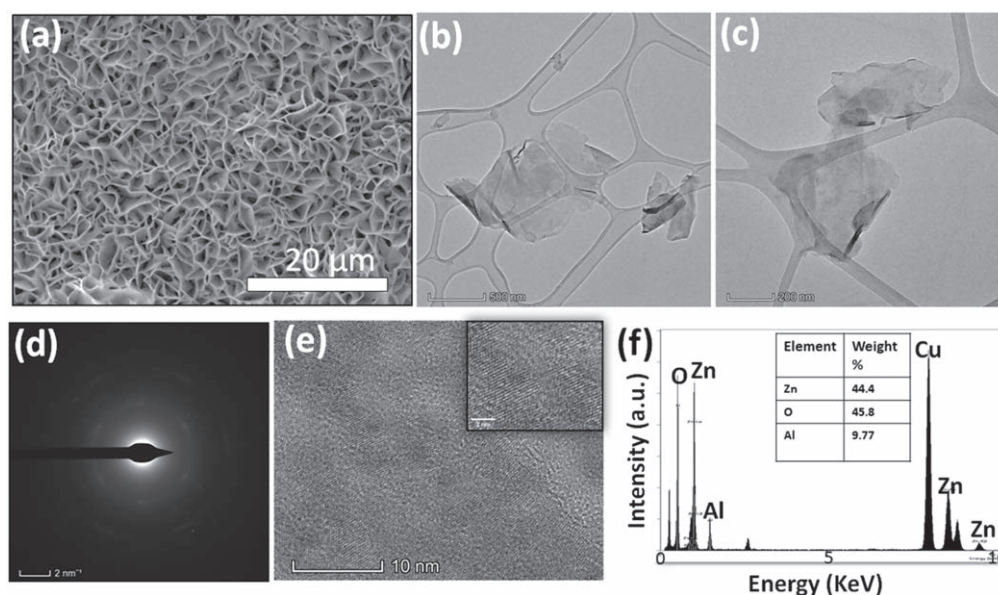


Figure 2. (a) SEM image of the ZnO nanosheets grown on aluminium substrate, (b)–(c) Individual ZnO nanosheet TEM images, (d) SAED pattern, (e) HRTEM image of the ZnO nanosheet, (f) EDX spectrum of the ZnO nanosheet.

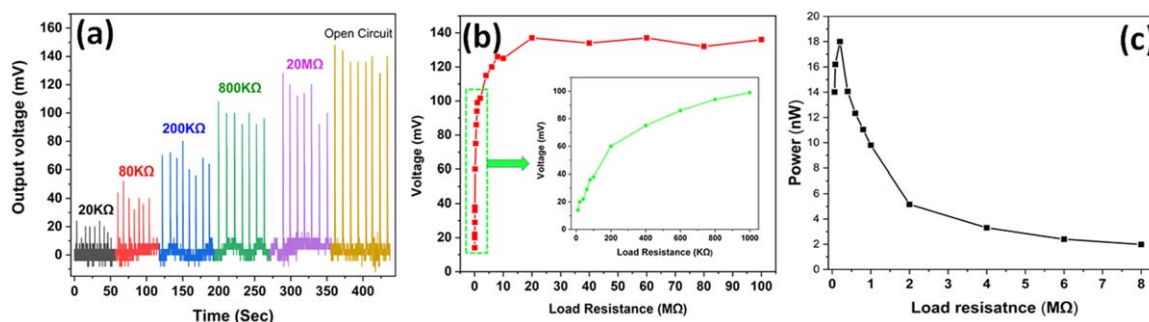


Figure 3. (a) Response of the nanogenerator under stable finger tapping with different load resistances, (b) Variation of output voltage under external variable load resistance under uniform finger tapping, (c) Power profile of the nanogenerator with load resistance variation.

a higher degree of deformation of nanosheets compared to twisting PENG.

Further, PENG response was recorded under different frequencies/speeds of finger tapping such as low (1 Hz), medium (3 Hz), high (6 Hz). The response of the PENG for the different frequencies of finger tapping is shown in figure 4(c). It is clear that reliable and stable output is observed under different finger-tapping frequencies. The slight decrement in the open-circuit voltage at higher frequencies is due to the inability to apply the same finger tapping force. Further, PENG's pressure sensing application is tested against different finger-tapping pressures (low, medium, and high). Figure 4(d) shows the response of the PENG for different finger-tapping pressures. It is evident from figure 4(d) that PENG output voltage increased with the increase of applied finger pressure. The output voltage has been increased from ~ 76 mV to ~ 145 mV with the increase of finger tapping pressure. The PENG can be further implemented for practical pressure sensing if the output of the nanogenerator is calibrated against known pressure with a load cell.

Long term stability test has been conducted to confirm the mechanical reliability and endurance of the PENG. Figure 5(a) shows the response of the nanogenerator under 1440 cycles of repetitive finger-tapping with a few seconds break of every 250 finger tapings. The fabricated PENG has shown excellent response over all the cycles. The variation in the output voltage within the 1440 cycles is due to the variation in the applied pressure by manual finger tapping. The generated output voltage from PENG does not alter much even after 1440 cycles. The stability of PENG output was tested at different times, such as immediately after the device fabrication, after 3, 6, and 12 months as shown in figure 5(b). These results show that the PENG device can work for a longer period without any degradation in the response. The long-term stability, mechanical reliability, and endurance of the PENG were studied only in few reports in the literature, and our results well match with the literature [24, 37]. It is evident from figure 5(b) that the response of the PENG is exceptionally stable over one year. It is concluded that PENG is very stable in the aspect of material and response. The high stability of the ZnO nanosheet-based PENG is attributed to the morphologically networked ZnO nanosheets and the high

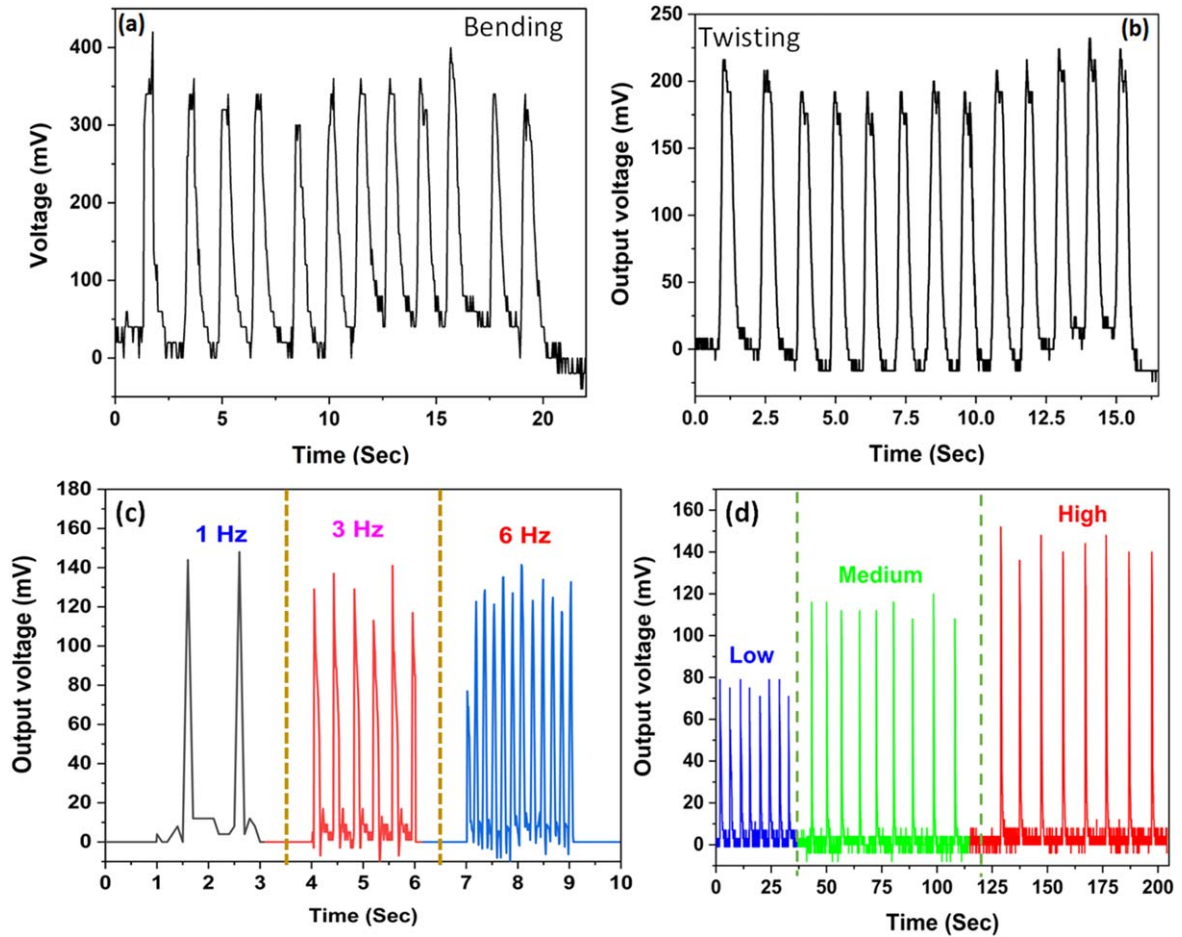


Figure 4. Open circuit voltage of the nanogenerator under (a) repeated bending of the device, (b) repeated twisting of the device, (c) different frequencies of finger tapping, (d) finger tapping with different impact magnitudes (low, medium, and high).

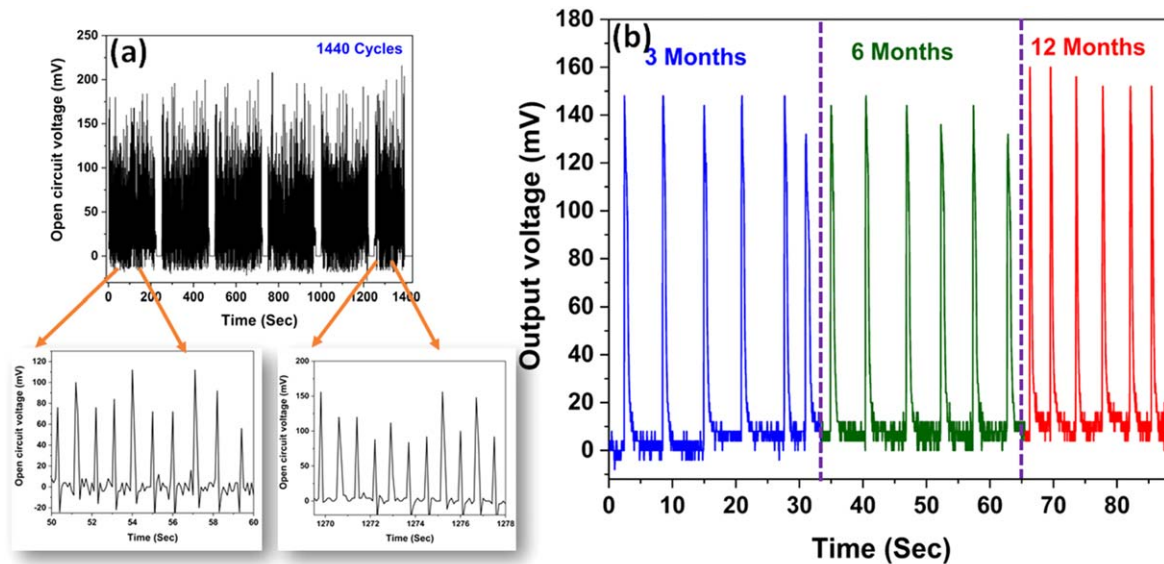


Figure 5. (a) Response of the nanogenerator under cyclic tests of 1440 finger tapping cycles, (b) Response of the nanogenerator against finger tapping at different points of time such as 3 months, 6 months, and 12 months after the device fabrication.

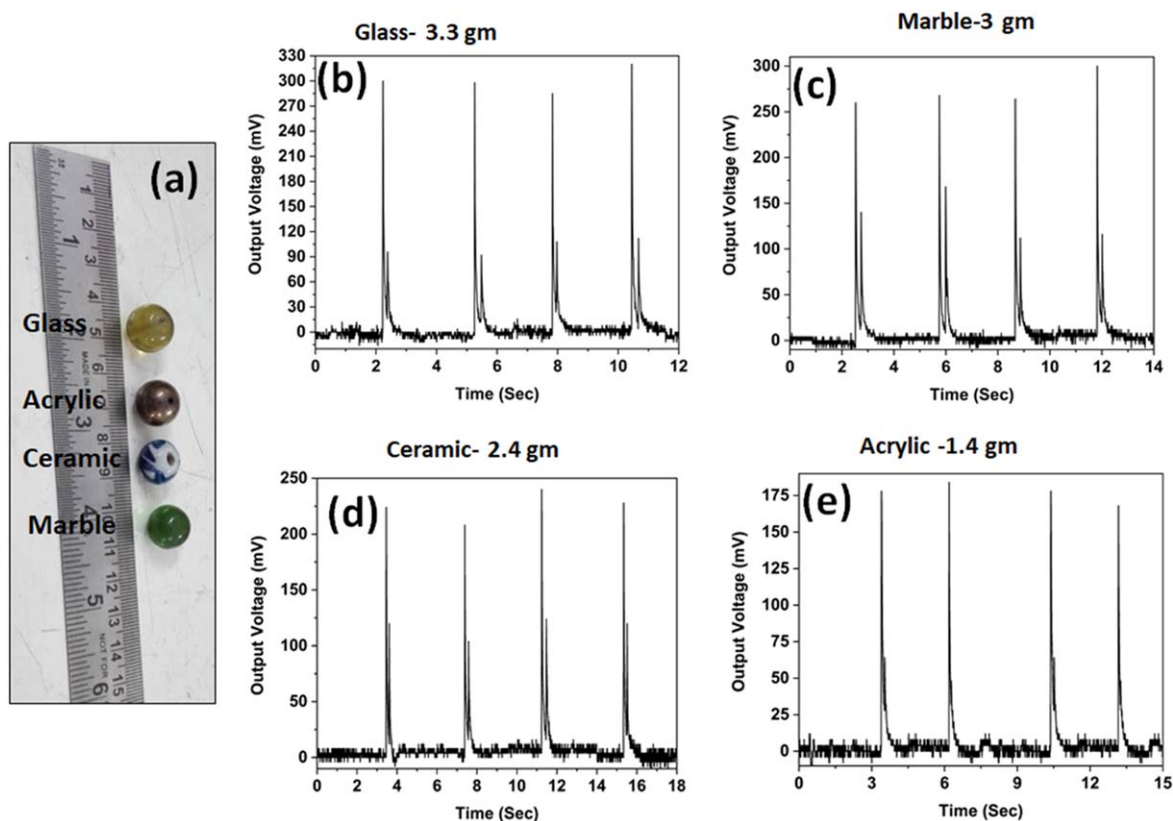


Figure 6. (a) Photographs of the different balls; Output voltage of nanogenerator for the different magnitudes of impacts by (b) glass, (c) marble, (d) ceramic, (e) acrylic balls.

mechanical strength of nanosheets as reported in the literature [21].

Figure 6(a) shows the photographs of different spherical balls, namely glass, acrylic, ceramic, marble (top to bottom). The ball drop test has been performed a minimum of four times for a fixed height of 35 cm for each ball for accuracy and repeatability (see multimedia file). Figures 6(b)–(d) show the nanogenerator's response for different impacts applied by the glass, marble, acrylic, and ceramic material balls, respectively. When the test ball was dropped from the height, it exerts a force on the ZnO nanosheets of the nanogenerator. The force applied by the impact causes the mechanical deformation of nanosheets and produces a piezoelectric voltage. The output voltage was decreased from an average value of 300 mV to 176 mV with a decrease in the mass (weight) of balls. The density of material (ball) depends on the mass of the material and volume. Since the volumes of all balls are the same in our experiment, the density variation of different balls depends on the mass of the balls. Therefore, we can conclude that the change in the magnitude of the output voltage is a function of the material's density. Higher magnitude output corresponds to the higher density material. This study will be useful in the preparing database for the materials of different densities provided all materials are in the same shape and diameter. This database can be used for finding the density of the unknown materials using scaling analysis.

Figure 7(a) shows the variation of output voltage in response to the impact applied by different balls of equal

diameter but with a different mass. The magnitude of the impact depends on its mass and drop height. As the drop height is constant in our case, the magnitude of the impact depends only on the mass of the balls. The response output voltage was increased proportionally to the increase in the magnitude of impact due to different masses of balls as expected.

Figure 7 (b) shows the variation of output voltage in response to the impact applied by the same acrylic ball, dropped from different heights of 5 cm, 10 cm, 20 cm, and 35 cm. The magnitude of the impact depends on its mass and drop height. As the mass of the ball is constant in this case, the magnitude of the impact depends only on drop height. The response output voltage is increased proportionally to the increase in the impact due to different drop heights of the ball as expected. The above results will be useful in non-destructive material discrimination in small and medium-scale industries.

4. Conclusions

In conclusion, the ZnO nanosheets are grown on conducting aluminium substrate by a cost-effective hydrothermal method at 80 °C in a hot air oven. The SEM and TEM studies confirm the uniform growth of nanosheets, and the size of sheets is in the range of $\sim 0.5\text{--}1\ \mu\text{m}$. The polycrystalline nature of the individual nanosheets is confirmed with TEM studies. A

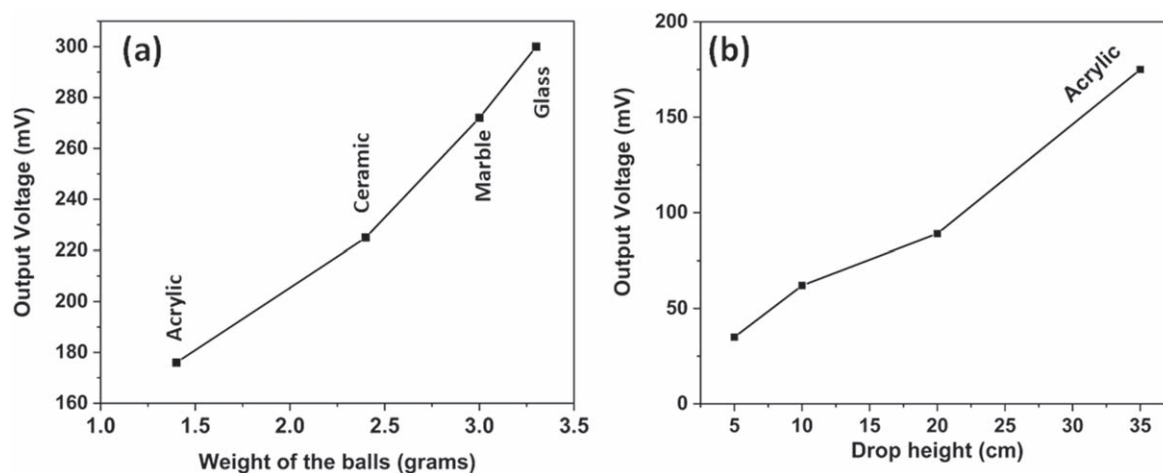


Figure 7. (a) Variation of output voltage with different weights of the balls, (b) Variation of output voltage for acrylic ball dropped from different heights.

piezoelectric nanogenerator is fabricated using two dimensional ZnO nanosheet network and its different characteristics are studied. The fabricated nanogenerator was demonstrated for the mechanical energy harvesting using bending and twisting motions. The output voltages of ~ 350 mV and 200 mV were observed for bending and twisting movements of the device. The maximum output power of 18 nW was obtained at the load resistance of 200 Kohms with 60 mV output voltage. Similarly, the fabricated nanogenerator was demonstrated for the low, medium and high-pressure sensing applied by the finger. The output voltages of ~ 76 mV, 100 mV, and 145 mV were observed for low, medium, and high pressures applied by the finger. The PENG has shown excellent stability and repeatability of its response to finger tapping over 1440 cyclic tests, over a period of one year. Finally, the fabricated nanogenerator also demonstrated the possible application of material discrimination by a ball drop test. The output voltage generated for each ball discriminating them based on their density. The nanogenerator output can be calibrated using different densities of materials and can be used as a reference database for the density of the materials. The present results open up a new strategy for material discrimination in a non-destructive way with reference to a calibrated database. Further, a touch sensor, electronic skin applications can be explored from the reported nanogenerator in the future.

Acknowledgments

The authors are grateful to the funding agency SERB, DST, Govt. of India for kindly supporting the study reported in this paper, in the form of this project (ECR project No. # SERB/ECR/2016/000802).

The authors acknowledge the TEM facility, funded by a TPF Nanomission, GOI project at Centre for Nano and Soft Matter Sciences, Bengaluru.

References

- [1] Roy P, Kumar Sinha N, Tiwari S and Khare A 2020 A review on perovskite solar cells: evolution of architecture, fabrication techniques, commercialization issues and status *Sol. Energy* **198** 665–88
- [2] Mo X, Zhou H, Li W, Xu Z, Duan J, Huang L, Hu B and Zhou J 2019 Piezoelectrets for wearable energy harvesters and sensors *Nano Energy* **65** 104033
- [3] Zabek D and Morini F 2019 Solid state generators and energy harvesters for waste heat recovery and thermal energy harvesting *Therm. Sci. Eng. Prog.* **9** 235–47
- [4] Covaci C and Gontean A 2020 Piezoelectric energy harvesting solutions: a review *Sensors (Switzerland)* **20** 1–37
- [5] Lee H, Kim H, Kim D Y and Seo Y 2019 Pure piezoelectricity generation by a flexible nanogenerator based on lead zirconate titanate Nanofibers *ACS Omega* **4** 2610–7
- [6] Jeong C K, Lee J H, Hyeon D Y, Gyu K Y, Kim S, Baek C, Lee G J, Lee M K, Park J J and Il P K 2020 Piezoelectric energy conversion by lead-free perovskite BaTiO₃ nanotube arrays fabricated using electrochemical anodization *Appl. Surf. Sci.* **512** 144784
- [7] Manjula Y, Rakesh Kumar R, Swarup Raju P M, Anil Kumar G, Venkatappa Rao T, Akshaykranth A and Supraja P 2020 Piezoelectric flexible nanogenerator based on ZnO nanosheet networks for mechanical energy harvesting *Chem. Phys.* **533** 110699
- [8] Jamond N, Chrétien P, Gatilova L, Galopin E, Travers L, Harmand J C, Glas F, Houzé F and Gogneau N 2017 Energy harvesting efficiency in GaN nanowire-based nanogenerators: the critical influence of the Schottky nanocontact *Nanoscale* **9** 4610–9
- [9] Wu J M and Kao C C 2014 Self-powered pendulum and micro-force active sensors based on a ZnS nanogenerator *RSC Adv.* **4** 13882–7
- [10] Chen A, Zhang C, Zhu G and Wang Z L 2020 Polymer materials for high-performance triboelectric Nanogenerators *Adv. Sci.* **7** 2000186
- [11] Schmidt-Mende L and MacManus-Driscoll J L 2007 ZnO—nanostructures, defects, and devices *Mater. Today* **10** 40–8
- [12] Le A T, Ahmadipour M and Pung S-Y 2020 A review on ZnO-based piezoelectric nanogenerators: synthesis, characterization techniques, performance enhancement and applications *J. Alloys Compd.* **844** 156172
- [13] Mustapha S, Ndamitso M M, Abdulkareem A S, Tijani J O, Shuaib D T, Mohammed A K and Sumaila A 2019

- Comparative study of crystallite size using Williamson-Hall and Debye-Scherrer plots for ZnO nanoparticles *Adv. Nat. Sci. Nanosci. Nanotechnol.* **10** 045013
- [14] Wang Z L and Song J 2006 Piezoelectric nanogenerators based on zinc oxide nanowire arrays *Science* **312** 242–6
- [15] Wang X 2012 Piezoelectric nanogenerators—harvesting ambient mechanical energy at the nanometer scale *Nano Energy* **1** 13–24
- [16] Lin L, Hu Y, Xu C, Zhang Y, Zhang R, Wen X and Lin Wang Z 2013 Transparent flexible nanogenerator as self-powered sensor for transportation monitoring *Nano Energy* **2** 75–81
- [17] Zhao Y, Lai X, Deng P, Nie Y, Zhang Y, Xing L and Xue X 2014 Pt/ZnO nanoarray nanogenerator as self-powered active gas sensor with linear ethanol sensing at room temperature *Nanotechnology* **25** 115502
- [18] Yu A, Jiang P and Lin Wang Z 2012 Nanogenerator as self-powered vibration sensor *Nano Energy* **1** 418–23
- [19] Sinha N, Goel S, Joseph A J, Yadav H, Batra K and Kumar M 2018 Y-doped ZnO nanosheets: Gigantic piezoelectric response for an ultra-sensitive flexible piezoelectric nanogenerator *Ceram. Int.* **44** 8582–90
- [20] Wang Q, Yang D, Qiu Y, Zhang X and Song W 2018 Two-dimensional ZnO nanosheets grown on flexible ITO-PET substrate for self-powered energy-harvesting nanodevices *Appl. Phys. Lett.* **112** 063906
- [21] Gupta M K, Lee J H, Lee K Y and Kim S W 2013 Two-dimensional vanadium-doped ZnO nanosheet-based flexible direct current nanogenerator *ACS Nano* **7** 8932–9
- [22] Kim K H, Kumar B, Lee K Y, Park H K, Lee J H, Lee H H, Jun H, Lee D and Kim S W 2013 Piezoelectric two-dimensional nanosheets/anionic layer heterojunction for efficient direct current power generation *Sci. Rep.* **3** 2017
- [23] Duerloo K N, Ong M T and Reed E J 2012 Intrinsic piezoelectricity in two-dimensional materials *The Journal of Physical Chemistry Letters* **3** 2871–6
- [24] Lee Y, Kim S, Kim D, Lee C, Park H and Lee J 2020 Applied surface science direct-current flexible piezoelectric nanogenerators based on two-dimensional ZnO nanosheet *Appl. Surf. Sci.* **509** 145328
- [25] Joshi S, Hegde G M, Nayak M M and Rajanna K 2013 A novel piezoelectric thin film impact sensor: application in non-destructive material discrimination *Sensors Actuators A Phys.* **199** 272–82
- [26] Nyffenegger P A, Hinich M J, Ritter D and Hansen S 2004 Material discrimination using bispectral signatures *J. Acoust. Soc. Am.* **116** 1518–23
- [27] Nik S J, Meyer J and Watts R 2011 Optimal material discrimination using spectral x-ray imaging *Phys. Med. Biol.* **56** 5969–83
- [28] García-Allende P B, Conde O M, Cubillas A M, Jáuregui C and López-Higuera J M 2007 New raw material discrimination system based on a spatial optical spectroscopy technique *Sensors Actuators A Phys.* **135** 605–12
- [29] Gaddam V, Kumar R R, Parmar M, Yaddanapudi G R K, Nayak M M and Rajanna K 2015 Morphology controlled synthesis of Al doped ZnO nanosheets on Al alloy substrate by low-temperature solution growth method *RSC Adv.* **5** 13519–24
- [30] Cheng J P, Liao Z M, Shi D, Liu F and Zhang X B 2009 Oriented ZnO nanoplates on Al substrate by solution growth technique *J. Alloys Compd.* **480** 741–6
- [31] Cheng J P, Zhang X B and Luo Z Q 2008 Oriented growth of ZnO nanostructures on Si and Al substrates *Surf. Coatings Technol.* **202** 4681–6
- [32] Cao F, Li C, Li M, Li H, Huang X and Yang B 2018 Direct growth of Al-doped ZnO ultrathin nanosheets on electrode for ethanol gas sensor application *Appl. Surf. Sci.* **447** 173–81
- [33] Murillo G, Leon-Salguero E, Martínez-Alanis P R, Esteve J, Alvarado-Rivera J and Güell F 2019 Role of aluminum and HMTA in the hydrothermal synthesis of two-dimensional n-doped ZnO nanosheets *Nano Energy* **60** 817–26
- [34] Boughey F L, Davies T, Datta A, Whiter R A, Sahonta S L and Kar-Narayan S 2016 Vertically aligned zinc oxide nanowires electrodeposited within porous polycarbonate templates for vibrational energy harvesting *Nanotechnology* **27** 28LT02
- [35] Rafique S, Kasi A K, Kasi J K, Aminullah, Bokhari M and Shakoor Z 2020 Fabrication of silver-doped zinc oxide nanorods piezoelectric nanogenerator on cotton fabric to utilize and optimize the charging system *Nanomater. Nanotechnol.* **10** 1–12
- [36] Saravanakumar B and Kim S 2014 Growth of 2D ZnO Nanowall for energy harvesting application *The Journal of Physical Chemistry C* **118** 8831–6
- [37] Aminullah K A K, Najma B, Kasi J K, Rafique S and Bokhari M 2020 Fabrication of piezoelectric nanogenerator using 3D-ZnO nanosheets and optimization of charge storage system *Mater. Res. Bull.* **123** 110711
- [38] Kaur J and Singh H 2020 Fabrication and analysis of piezoelectricity in 0D, 1D and 2D Zinc Oxide nanostructures *Ceram. Int.* **46** 19401–7